C.P. No. 288
(18,260)
A.R.C. Technical Report

C.P. No. 288
(18,260)
A.R.C Technical Report

MINISTRY OF SUPPLY

AERONAUTICAL RESEARCH COUNCIL

CURRENT PAPERS

Low Speed Static and Fluctuating Pressure Distributions on a Cylindrical Body with a Square Flat Plate Airbrake

By

T. B. Owen

LONDON: HER MAJESTY'S STATIONERY OFFICE

1956

THREE SHILLINGS NET

Current Paper No. 288

U.D.C. No. 533.691.152.3:533.691.18

Technical Note No. Aero 2396

January, 1956

ROYAL AIRCRAFT ESTABLISHMENT

Low speed static and fluctuating pressure distributions on a cylindrical body with a square flat plate airbrake

by

T. B. Owen

SUMMARY

There is a very rapid increase both in the r.m.s. amplitude of the pressure fluctuations and in the area of the body affected, if the brake angle is increased beyond 50°. At the lower frequencies there is a large increase in amplitude between 40° and 50° which is associated with the appearance of a regular shedding of turbulent eddies. On the model used, with an average gap of about 27% of the length of the side of the brake, the shedding frequencies are in close agreement with those measured on an isolated plate at the smaller brake angles and slightly higher than on an isolated plate at the higher brake angles. The fluctuating pressures due to the brake are little affected by the distance of the brake from the tail of the body.

LIST OF CONTENTS

APPENDIX

TABLE

LIST OF ILLUSTRATIONS

1 Introduction

Measurements have been made of the mean values of the static pressure and the fluctuations in static pressure at the surface of a body fitted with an airbrake. Lift, drag and pitching moment measurements on the same model have been reported in Ref. 1.

2 Description of tests

The body was 4.5 in. in diameter with a parallel section about 6 diameters long, a faired nose and a bluff tail. The brake was a 3 in. square flat plate hinged on a line tangential to the body surface with a minimum gap of 0.2ℓ (where ℓ is the length of the side of the plate). A sketch of the model is given in Fig. 1. The equipment used to measure the pressure fluctuations is described in an Appendix.

The pressure pickup was buried in the body with the end of one pipe flush with the surface. The other pipe was connected to a length of 3/32 in. O.D. copper tubing leading to the outside of the tunnel.

It had been inferred from the measurements of Ref. 1 that the body static pressure distribution associated with the brake was practically unaffected by the distance of the brake from the tail of the body provided that this distance was greater than 3ℓ. The pressure pickup was therefore buried in the body 4ℓ ahead of the tail for most of the tests and the brake hinge position was varied from 3ℓ to 9ℓ.

At the higher brake angles it was found that the pressure fluctuations were still appreciable 5ℓ behind the brake hinge; at brake angles of 70° and 90° the field of measurement was therefore extended to 6.5ℓ by using the pickup 2.5ℓ ahead of the tail of the body.

In addition a few measurements were made with the pressure pickup at 0.5ℓ and 1.0ℓ ahead of the tail to discover whether the pressure fluctuations are affected by the proximity of the brake to the tail of the body.

The static pressure distributions behind the brake-hinge were measured using the pressure pickup but it was found more convenient to make the measurements ahead of the brake-hinge with a 'creeper' static tube connected to a manometer. For the latter tests the brake-hinge was fixed at 5.4ℓ ahead of the tail of the body.

The tests were made in the R.A.E. 4 ft × 3 ft wind tunnel in January and April 1955 at a wind speed of 140 ft/sec. The model was suspended from the roof of the tunnel by a single braced strut, with the rear of the model located by three wires attached to an axial spindle just aft of the bluff tail of the body (Fig. 1). The brake was always attached below the body, i.e. on the shorter axis of the tunnel. The off-axis pressure measurements were made by rotating the rear part of the body containing the pressure pickup about the longitudinal body axis.

The body axis was at zero incidence throughout.

3 Discussion of Results

The mean static and fluctuating pressure distributions on the body due to the brake are shown in Fig. 5. The mean static pressure (P) is given in terms of $\frac{1}{2}\rho U_o^2$ relative to the static pressure on the body without brake. The r.m.s. value of the static pressure fluctuation (p) is also given in terms of $\frac{1}{2}\rho U_o^2$; on the body without brake the value of $p/\frac{1}{2}\rho U_o^2$ was about 0.003. A blockage correction for the body only has been applied to all the results, amounting to 1.6% on $\frac{1}{2}\rho U_o^2$.

3.1 Flow characteristics

An examination of the flow with a wool tuft showed that, at a brake angle of 30°, the flow was still attached to the rear surface of the brake on the centre line and that there were two large trailing vortices from the tips. By 40° the flow had completely separated from the rear surface of the brake and there was a closed bubble containing a circulating flow behind the brake. Further increases in the brake angle did not alter the type of flow pattern but the bubble, which at 40° was small and well clear of the body, grew with increasing brake angle until at 90° it was of greater cross section than the brake and appeared to touch the body surface about 3ℓ behind the brake hinge.

3.2 Mean static pressure distribution

At a brake angle of 30° there is a large suction under the brake, associated with the high velocity through the gap. This suction is markedly reduced at 40° and as the angle is further increased the pattern remains similar but there is a gradual reduction in the suction behind the brake and an increase in the positive pressure ahead of the brake.

3.3 Pressure fluctuations

At a brake angle of 30° there is a high level of pressure fluctuation on the body immediately above the brake, associated with the rapid expansion of the passage between the brake and the body. The level of the fluctuations is much reduced at 40° brake angle when the flow has separated from the rear surface of the brake. Further increase in the brake angle gives a rapid increase both in the level of the pressure fluctuations and in the area of the body affected. As an illustration of this, the integral of the pressure fluctuation amplitude (above 0.01) and the area affected is plotted in Fig. 7 as a coefficient based on brake area. The curve rises very rapidly beyond a brake angle of 50°, although it must be emphasized that the quantity plotted does not represent the true buffeting excitation since no allowance has been made for the phasing of the fluctuations (which was not measured) or the curvature of the body surface.

3.4 Spectra of pressure fluctuations

Analyses were made of the pressure fluctuations at a number of points (shown in Fig. 5). The resulting spectra are shown in Fig. 6*. For convenience in discussing the results two frequency ranges are arbitrarily defined:

low frequency range $n < 0.1$**
high frequency range $n > 0.1$

At 30° brake angle, most of the energy is in the high frequency range. Between 40° and 50° there is an increase in low frequency amplitudes of nearly three times. Further increase of the brake angle adds energy mainly in the high frequency range, but there is also a steady increase in the energy at low frequency.

---

* The ordinate used is $\sqrt{nF(n)}$ which has the advantage that the r.m.s. value of the pressure fluctuation in a small band of frequency is approximately equal to the appropriate value of $\sqrt{nF(n)}$ multiplied by the square root of the bandwidth ratio.

** For example, for a brake 3 ft square at 1000 ft/sec, $n = 0.1$ corresponds to a frequency of 33 c.p.s.

The large increase in low frequency excitation between 40° and 50° is associated with the appearance of a regular shedding of turbulent eddies (indicated by the sharp peaks* in the spectra) in the wake. The value of n at which shedding occurs is known as the Strouhal number. This is plotted in Fig. 8 together with the values for isolated plates reported in Ref. 1. It is apparent that with the gap used on the present model, the presence of the body has little effect on the Strouhal number, except at brake angles above about 60° when the presence of the body increases the shedding frequency slightly.

It is of interest to note that at 90° brake angle the spectrum measured off centre (Fig. 6(e) spectrum D) shows the shedding frequency peak very strongly, while the centre line spectra (B and C) show little sign of it and the small peak in centre line spectrum A is at twice the shedding frequency. This suggests that at a brake angle of 90° the fluctuations in flow associated with the shedding are predominantly lateral.

3.5 Effect of the proximity of the brake to the tail of the body

All of the results discussed so far have referred to tests in which the brake hinge line was at least 4ℓ ahead of the tail of the body, and the results should be independent of increased body length behind the brake. A few tests were made to check the effect on the pressure fluctuations of reducing the length of body behind the brake. The rearmost position of the pickup in these experiments was 0.5ℓ ahead of the tail of the body and the rearmost position of the brake was 1.5ℓ ahead of the tail. Details of the positions tested and the results obtained are given in Table I. It will be seen that the effect of reducing the length of body behind the brake hinge is generally small.

4 Conclusions

There is a rapid increase both in the r.m.s. amplitudes of the pressure fluctuations and in the area of the body affected, if the brake angle is increased above 50°. In the low frequency range (values of n below 0.1) there is a large increase in amplitude between 40° and 50° brake angle, which is associated with the appearance of a regular shedding of turbulent eddies. The value of n at which shedding occurs (Strouhal number) varies from 0.25 at 50° to 0.13 at 90°. These numbers are in fair agreement with those for an isolated plate, although the frequency of shedding is increased slightly due to the presence of the body at the higher brake angles. The pressure fluctuations due to the brake are not much affected by the distance of the brake from the tail of the body.

The mean static pressure distributions on the body show a positive peak ahead of the brake and a negative peak behind. These peak values vary from 0.1 q_o and -1.0 q_o at 30° brake angle to +0.6 q_o and -0.6 q_o at 90°. There is no obvious connection between the mean and fluctuating static pressure distributions in that the pressure fluctuation maxima do not in general correspond either to static pressure maxima or minima or to maximum static pressure gradient, although at the higher brake angles there is some local increase in the pressure fluctuations in the area of maximum pressure recovery gradient.

Further tests to investigate the effect of gap are to be made. The brake will be fitted on a flat-plate wing so that the gap can be defined more easily than on the cylindrical body.

---

* The shapes (including the heights) of the peaks in the spectra are determined by the characteristics of the analyser. Strictly, the results should be presented in the form of the continuous spectrum and the r.m.s. value of the fluctuation at the single frequency. For the present purpose it is sufficient to recognise the existence of peaks.

LIST OF SYMBOLS

θ = angle of brake relative to body axis

ℓ = length of side of brake

d = diameter of body

X = distance of brake hinge line from tail of body

x = distance of pressure pickup behind brake hinge

η = distance of pressure pickup from brake centre line measured along body surface

U_o = tunnel speed (corrected for body blockage of 0.8%)

f = frequency (cycles/second)

$n = \frac{f\ell}{U_o}$ = non dimensional frequency parameter

Δn = analyser bandwidth expressed non dimensionally

$q_o = \frac{1}{2}\rho U_o^2$

P = mean static pressure at a point on the body surface

$P + p'$ = instantaneous static pressure

$p^2 = \overline{p'^2}$ = mean square value (with respect to time) of static pressure fluctuations

Δp^2 = mean square value of static pressure fluctuation passed by analyser

$\epsilon_A = \frac{\Delta n}{n} = \frac{\text{analyser bandwidth (cycles/sec)}}{\text{tuned frequency (cycles/sec)}} = 0.1$

= analyser bandwidth ratio

$F(n)$ = Spectrum function (see Appendix)

REFERENCES

No.	Author	Title, etc.
1	R. Fail, T.B. Owen, R.C.W. Eyre	Preliminary low speed wind tunnel tests on flat plates and air-brakes: flow, vibration and balance measurements. C.P.251. January, 1955.
2	M.O.W. Wolfe	The measurement of fluctuating fluid pressures. Aircraft Engineering. Vol. 21. No. 250. December, 1949.
3	H. Schuh and D. Walker	Wide range amplifier for turbulence measurements with adjustable upper frequency limit. C.P. 198. August, 1953.

APPENDIX

Method of measuring fluctuating pressures

The pressure pickup (Fig. 3) was of capacity type, developed from an original design by Wolfe[2]. A block diagram of the associated equipment is given in Fig. 2. The analyser was of constant-percentage-bandwidth type (bandwidth = 0.1 × tuned frequency) with a range from 2.5 to 750 c.p.s. The final amplifier is described in Ref. 3.

With this equipment measurements were made of the mean square of the total output of the pickup, p^2. Measurements were also made of the mean square of the analyser output, Δp^2, over a range of frequency, f, or, in non-dimensional form, $n = f\ell/U_o$. The spectrum function F(n) is defined so that F(n) dn is the contribution to $p^2/q_o{}^2$ of frequencies between n and n + dn. Thus, if the analyser bandwidth is small,

$$F(n) = \Delta p^2/q_o{}^2 \, \Delta n$$

and

$$n\,F(n) = \Delta p^2/q_o{}^2 \, \varepsilon_A \qquad \text{approximately}$$

For the analyser used, $\varepsilon_A = \frac{\Delta n}{n}$ was roughly constant and equal to 0.1.

The mean square value of the pressure fluctuation $(p_{1,2})^2$ contained in the band of frequency between n_1 and n_2 is given by

$$(p_{1,2})^2/q_o{}^2 = \int_{n_1}^{n_2} F(n)\, dn$$

$$= \int_{n_1}^{n_2} n\,F(n)\, d(\log n)$$

and

$$p^2/q_o{}^2 = \int_{n=0}^{n=\infty} n\,F(n)\, d(\log n)$$

An example of the accuracy obtained with this equipment is shown in Fig. 4. These measurements were made, during the development of the pickup, on the rear wall of a rectangular cavity in a cylindrical body.

Further development of the equipment is proceeding so that measurements can be made at higher frequencies. This will enable tests to be made at higher speeds and on smaller models. A Muirhead PAMETRADA wave analyser has been obtained with a frequency range from 2 c.p.s. to 21 kc.p.s. The design of high frequency pickups is being considered; these will probably have flush diagrams about 0.5 in. in diameter.

TABLE I

Values of p/q_o on brake centre line

θ°	$\frac{x}{\ell}$	$\frac{X}{\ell}$				
		5.5	5.0	4.5	2.0	1.5
30	0.5	-	-	0.097	-	0.107
	1.0	-	0.069	-	0.077	0.068
	1.5	0.035	-	-	0.040	-
40	0.5	-	-	0.042	-	0.046
	1.0	-	0.037	-	0.036	0.039
	1.5	0.032	-	-	0.029	-
50	0.5	-	-	0.046	-	0.045
	1.0	-	0.052	-	0.051	0.051
	1.5	0.074	-	-	0.052	-
70	0.5	-	-	0.037	-	0.038
	1.0	-	0.051	-	0.052	0.051
	1.5	0.068	-	-	0.061	-
90	0.5	-	-	0.046	-	0.034
	1.0	-	0.061	-	0.067	0.051
	1.5	0.112	-	-	0.095	-

θ = Brake angle
ℓ = Length of side of brake
x = Distance of pickup behind brake hinge
X = Distance of brake hinge from tail of body

Wt.2078.C.P.288 - K3 - Printed in Great Britain

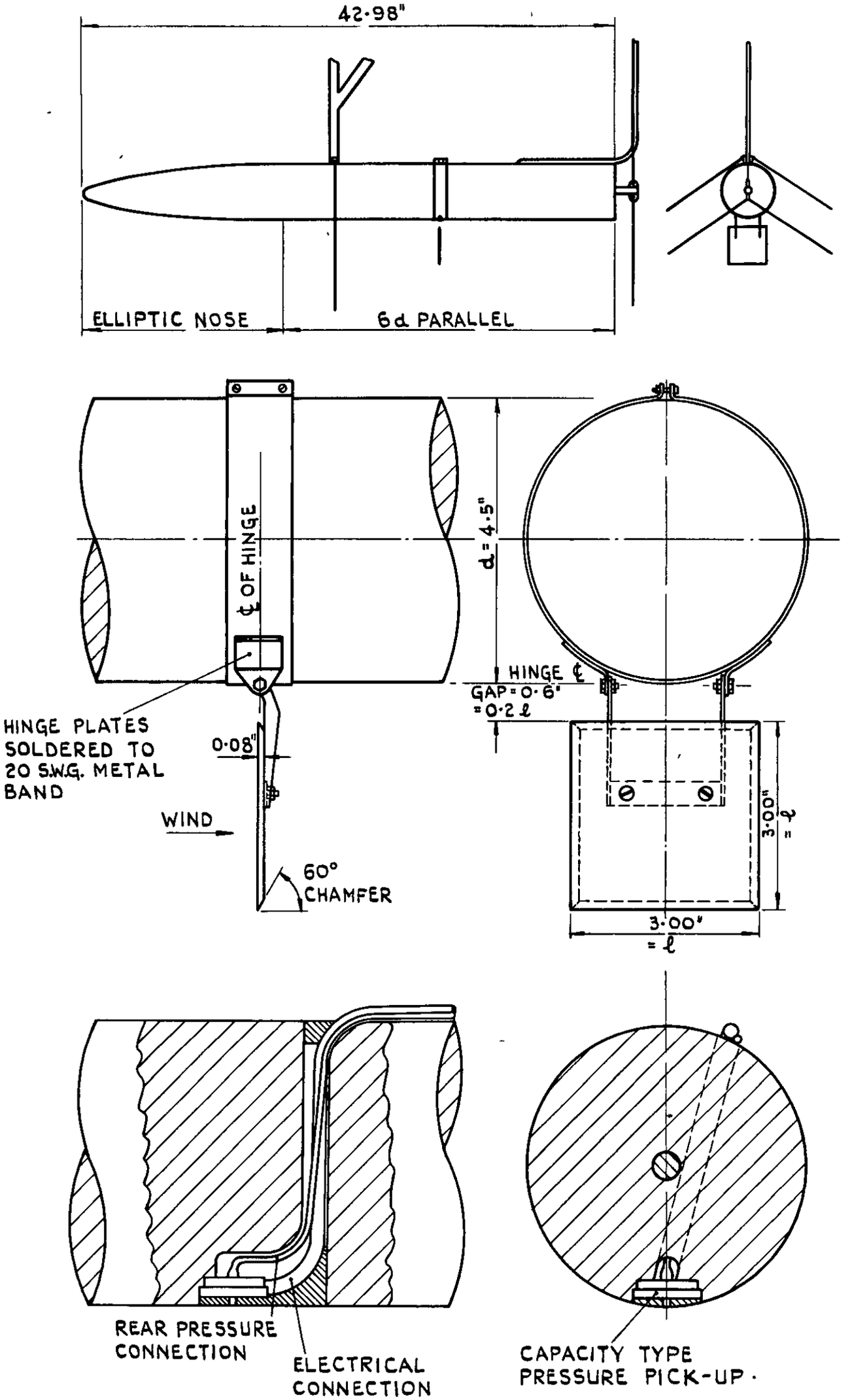

FIG.1. DETAILS OF MODEL.

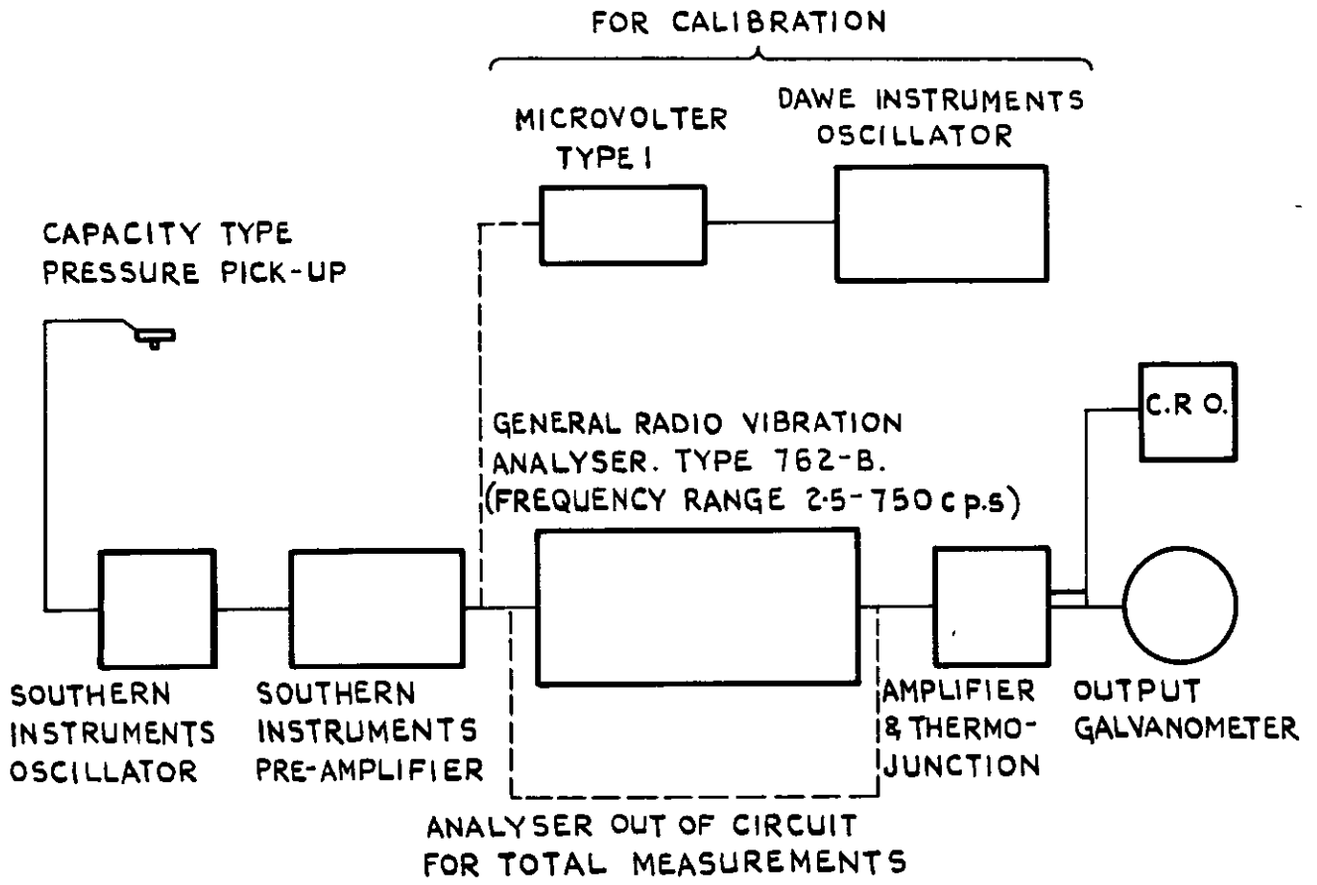

FIG.2. GENERAL ARRANGEMENT OF APPARATUS FOR MEASUREMENT OF PRESSURE FLUCTUATIONS.

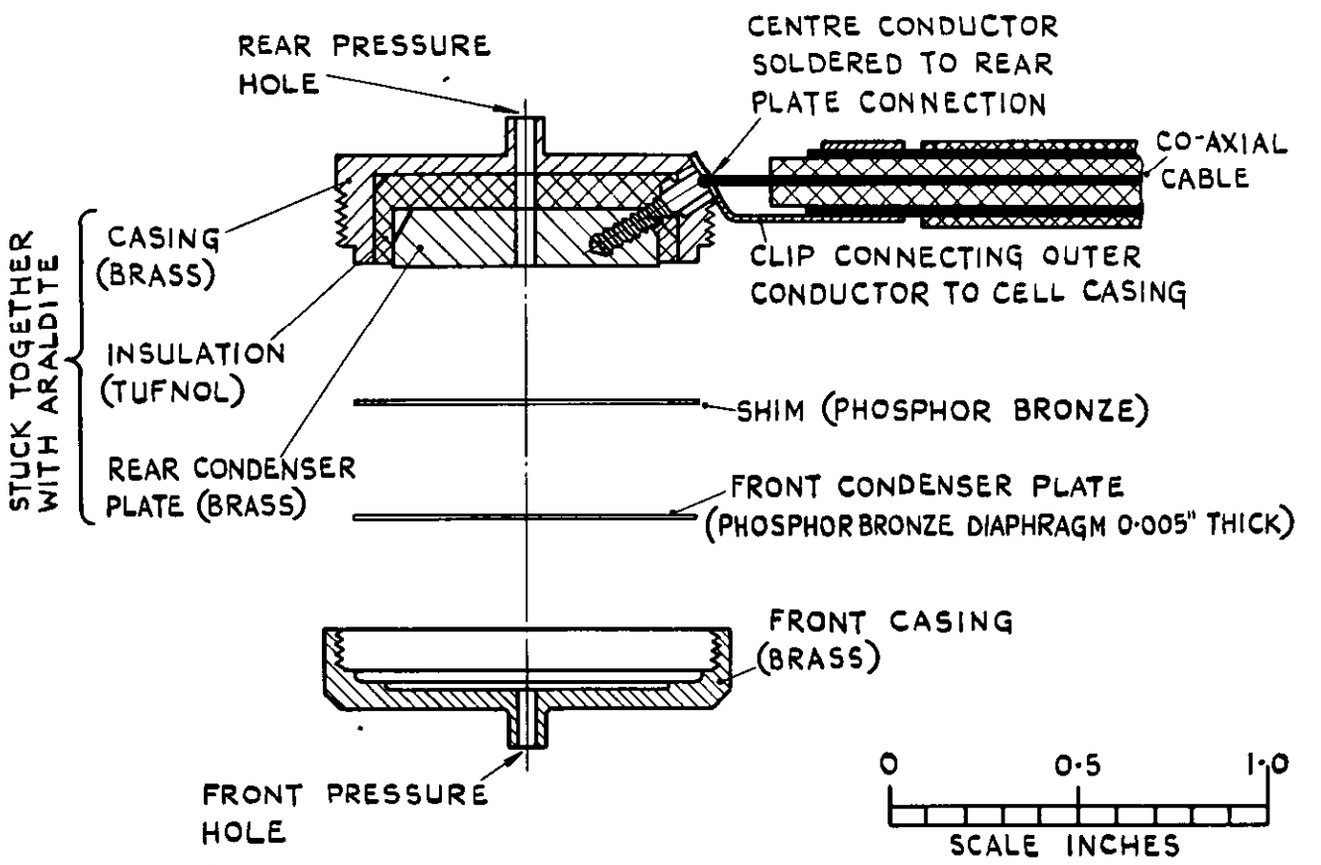

FIG.3. "EXPLODED" SECTION OF CAPACITY TYPE PRESSURE PICK-UP.

(SENSITIVITY ADJUSTED BY VARYING THICKNESS OF SHIM)

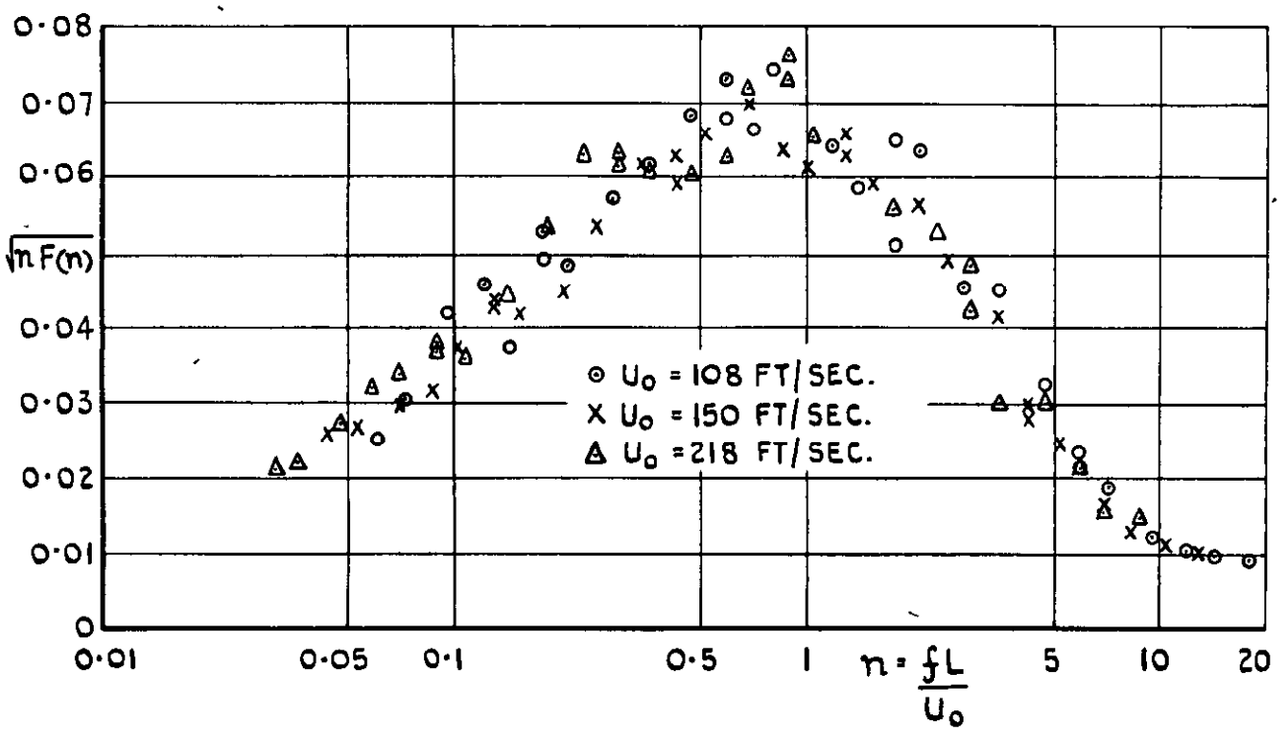

U_0 = FREE STREAM VELOCITY

f = FREQUENCY (CYCLES/SEC.)

Δp^2 = MEAN SQUARE OUTPUT OF ANALYSER

$$\epsilon_A = \frac{\text{ANALYSER BANDWIDTH (CYLES/SEC.)}}{\text{TUNED FREQUENCY (CYCLES/SEC.)}} = 0.100$$

L = LENGTH OF CAVITY

$$n = \frac{fL}{U_0}$$

$$n F(n) = \frac{\Delta p^2}{q_0^2 \epsilon_A}$$

R.M.S. VALUE OF THE PRESSURE FLUCTUATION IN A SMALL BAND OF FREQUENCY IS EQUAL TO $\sqrt{n F(n)}$ MULTIPLIED BY THE SQUARE ROOT OF THE BANDWIDTH RATIO

FIG. 4. EXAMPLE OF PRESSURE FLUCTUATION MEASUREMENTS ON REAR WALL OF RECTANGULAR CAVITY IN A CYLINDRICAL BODY. (SEE APPENDIX).

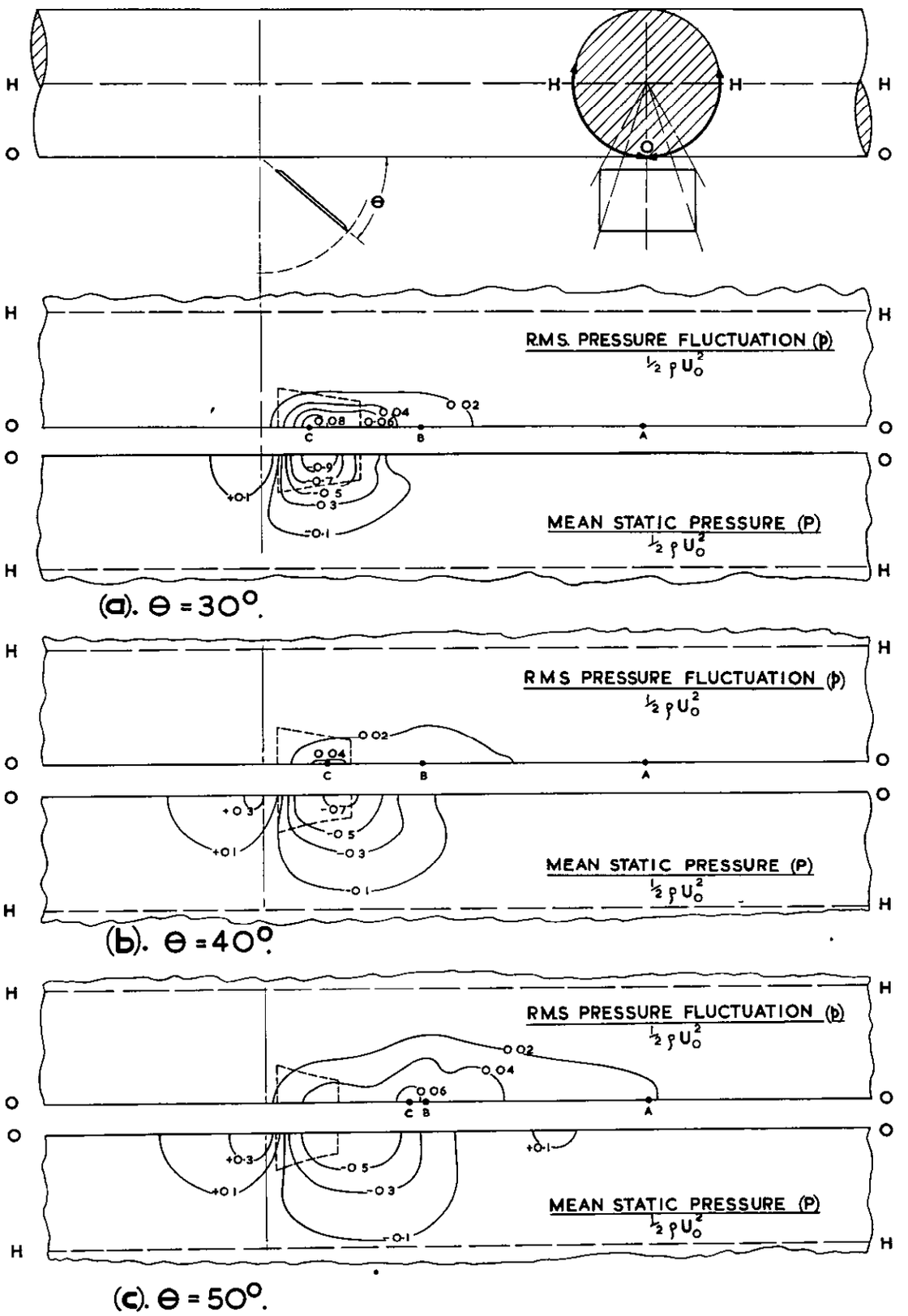

FIG.5 (a-c). FLUCTUATING AND STATIC PRESSURE DISTRIBUTIONS ON BODY SURFACE.

CONTOURS AND PROJECTED BRAKE AREA SHOWN ON DEVELOPED BODY SURFACE.
⊕ INDICATES POINTS AT WHICH SPECTRA HAVE BEEN MEASURED

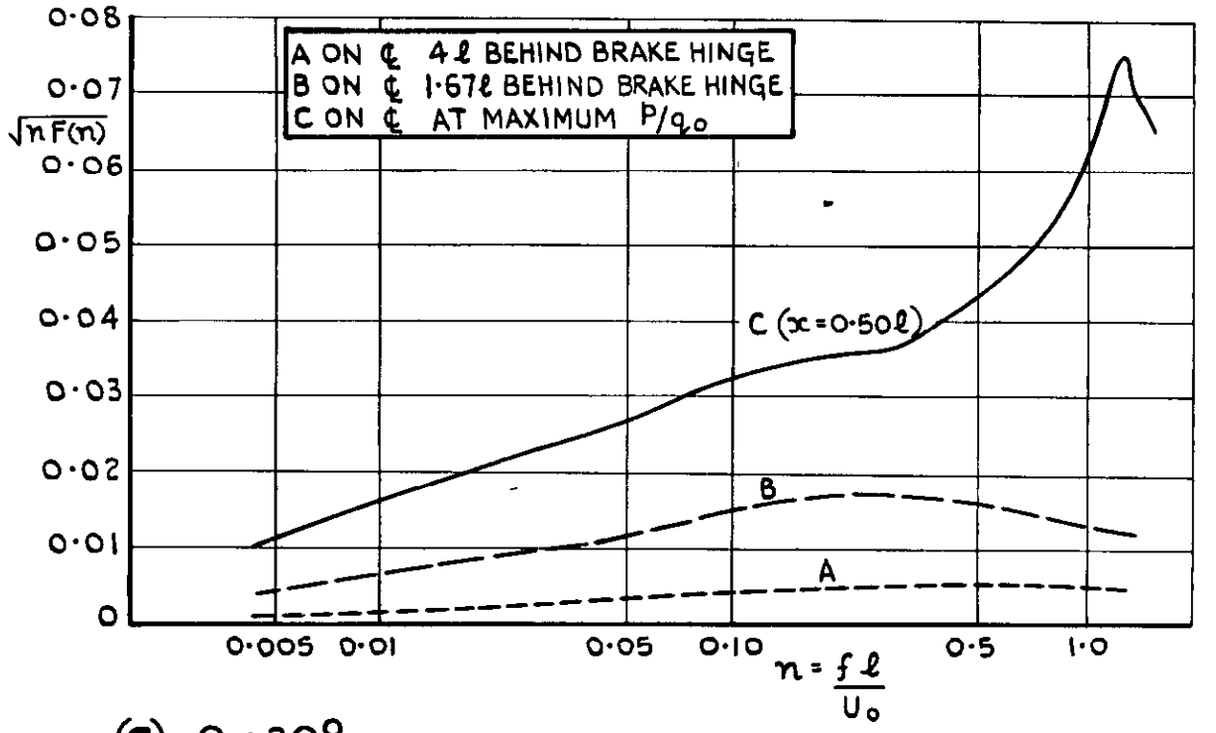

(a). $\Theta = 30^{\circ}$.

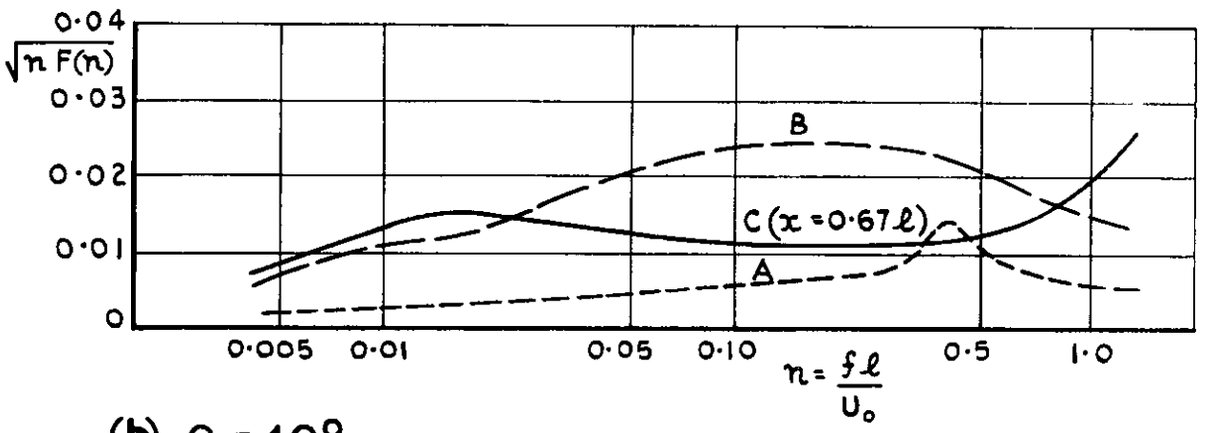

(b). $\Theta = 40^{\circ}$.

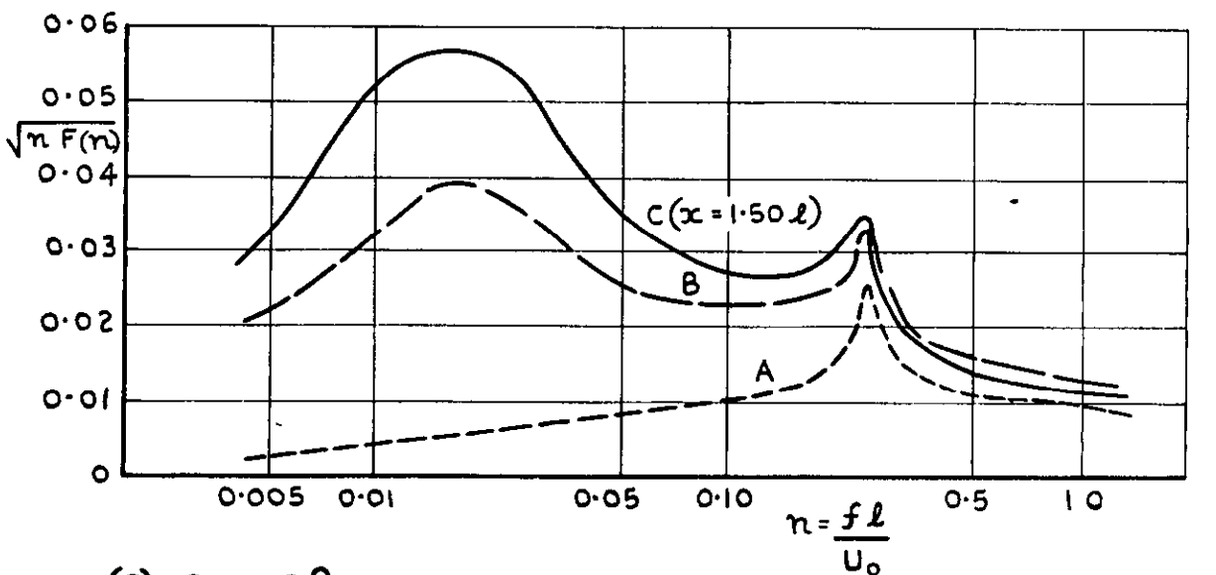

(c). $\Theta = 50^{\circ}$.

FIG. 6 (a-c). PRESSURE FLUCTUATION SPECTRA MEASURED AT POINTS INDICATED IN FIG. 5 (a-c).

x = DISTANCE OF PRESSURE PICK-UP BEHIND BRAKE HINGE-LINE.

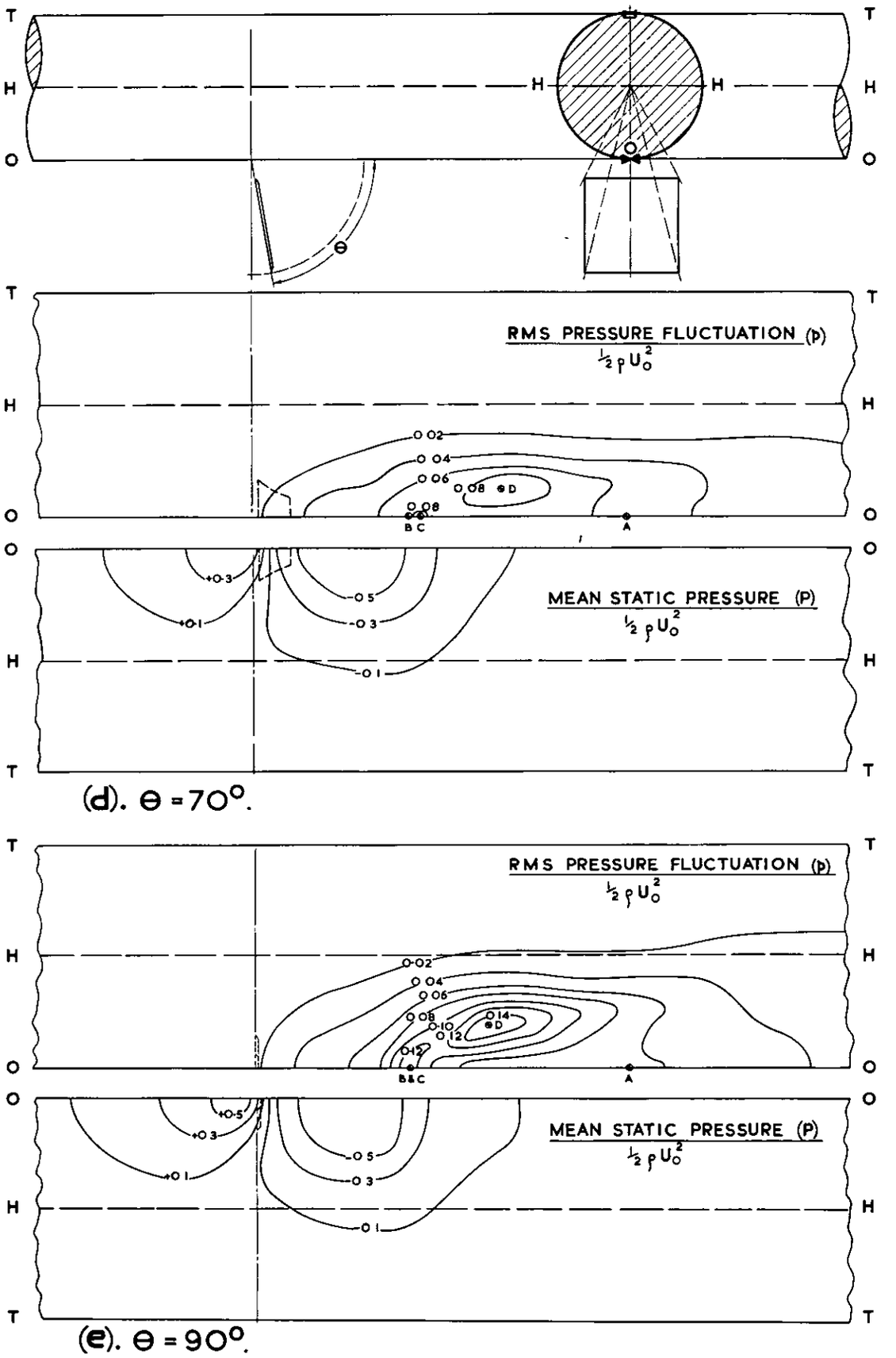

FIG.5(d&e). FLUCTUATING AND STATIC PRESSURE DISTRIBUTIONS ON BODY SURFACE.

CONTOURS AND PROJECTED BRAKE AREA SHOWN ON DEVELOPED BODY SURFACE.
⊕ INDICATES POINTS AT WHICH SPECTRA HAVE BEEN MEASURED.

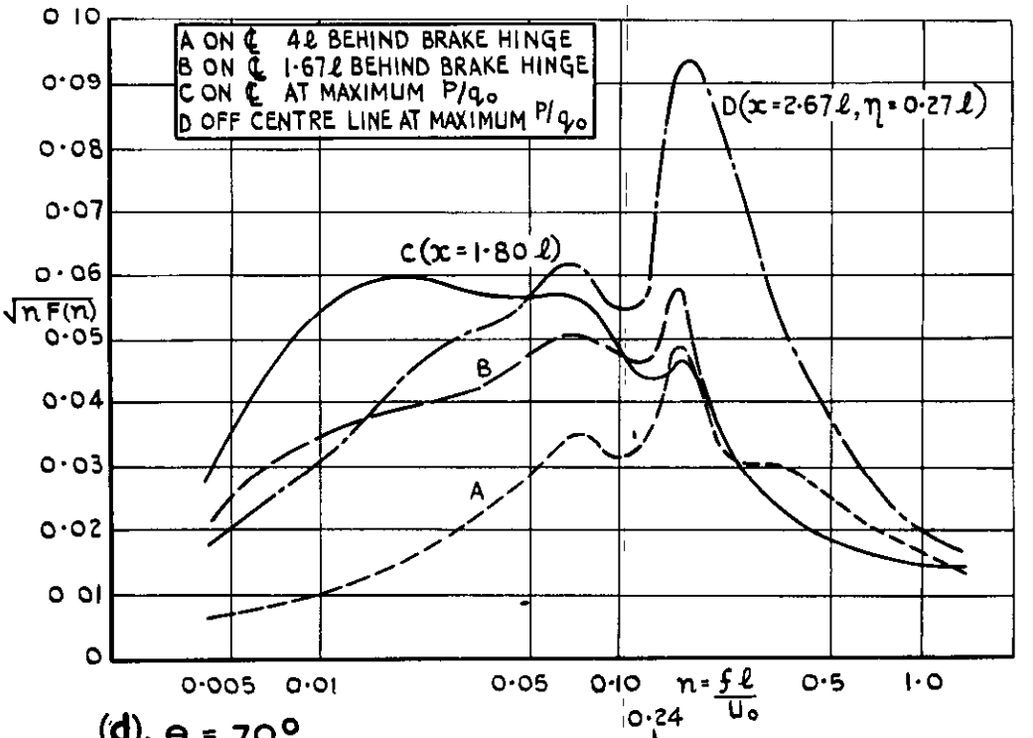

(d). θ = 70°.

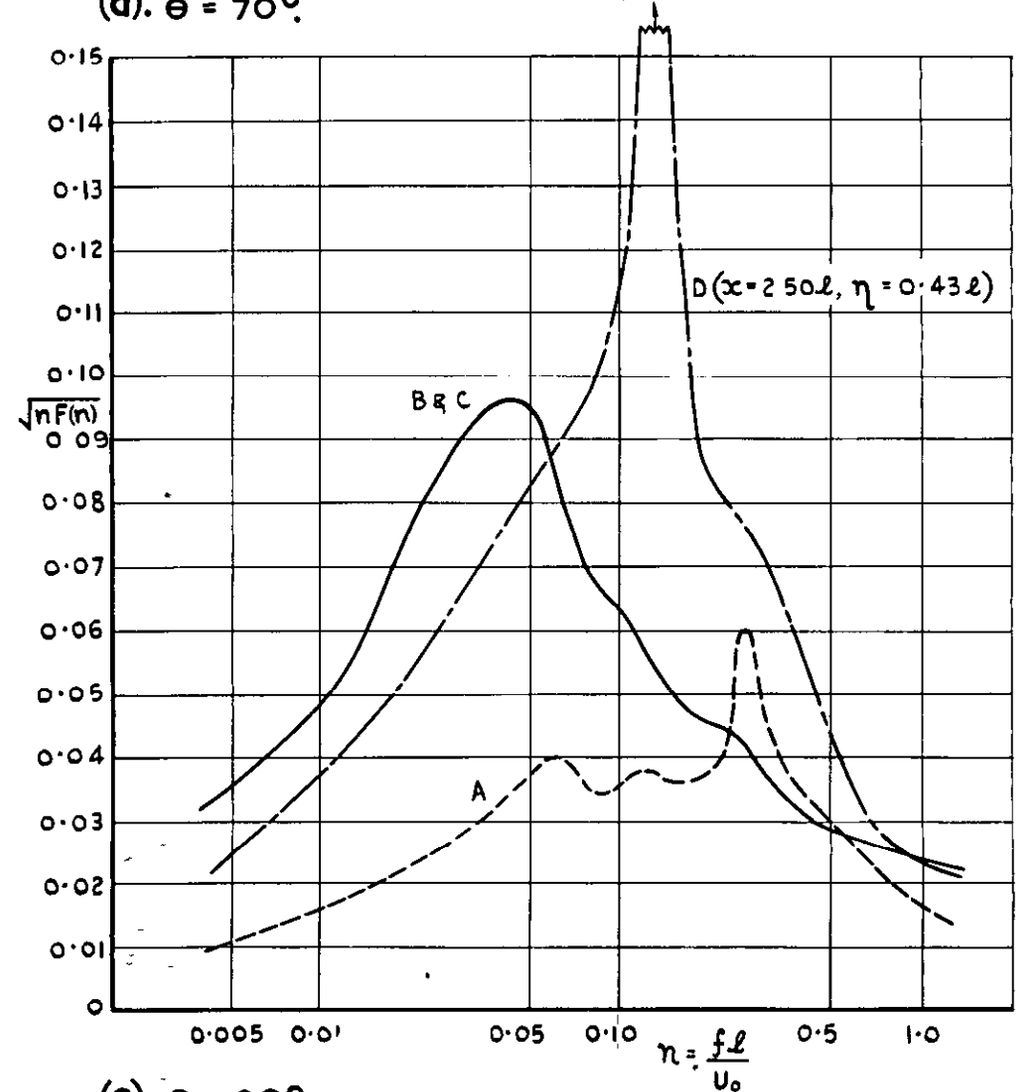

(e). θ = 90°.

FIG. 6 (d & e). PRESSURE FLUCTUATION SPECTRA MEASURED AT POINTS INDICATED IN FIG. 5 (d & e).

x = DISTANCE OF PRESSURE PICK-UP BEHIND BRAKE HINGE-LINE

η = DISTANCE OF PRESSURE PICK-UP FROM ℄ MEASURED ROUND BODY SURFACE

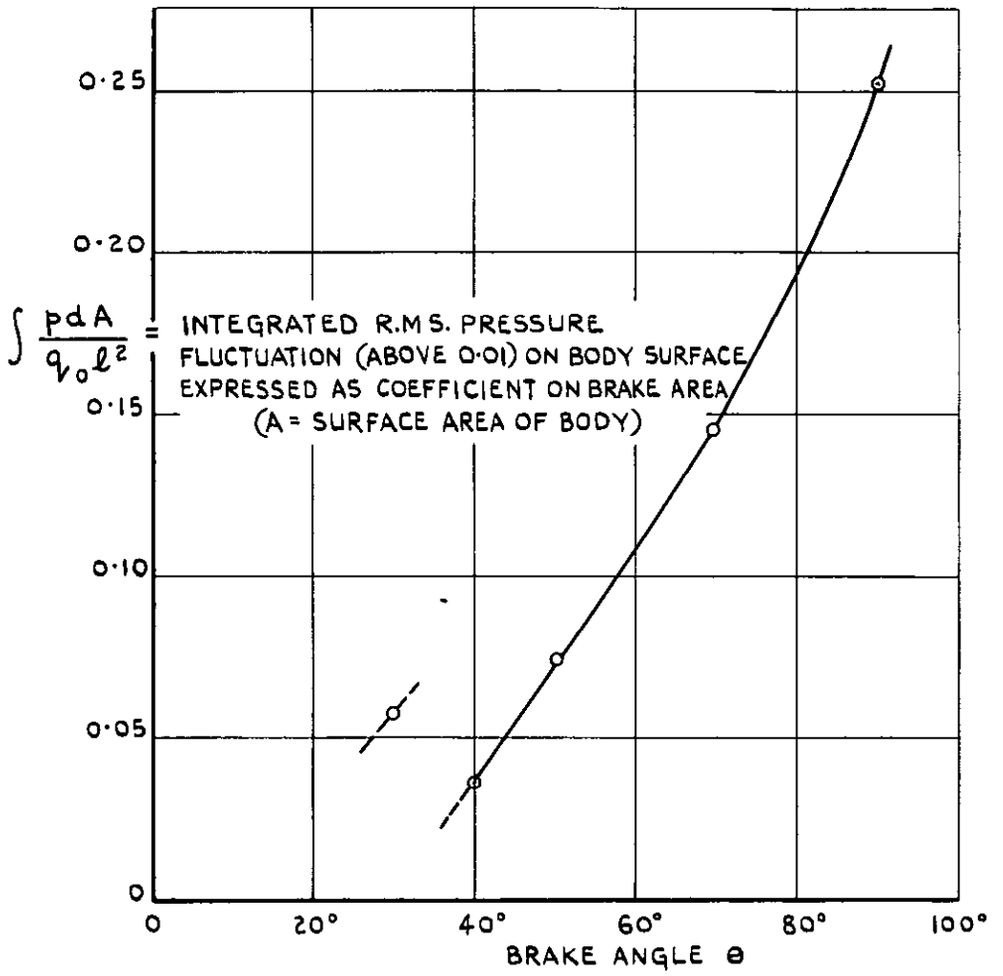

FIG.7. EFFECT OF BRAKE ANGLE ON PRESSURE EXCITATION ON BODY.

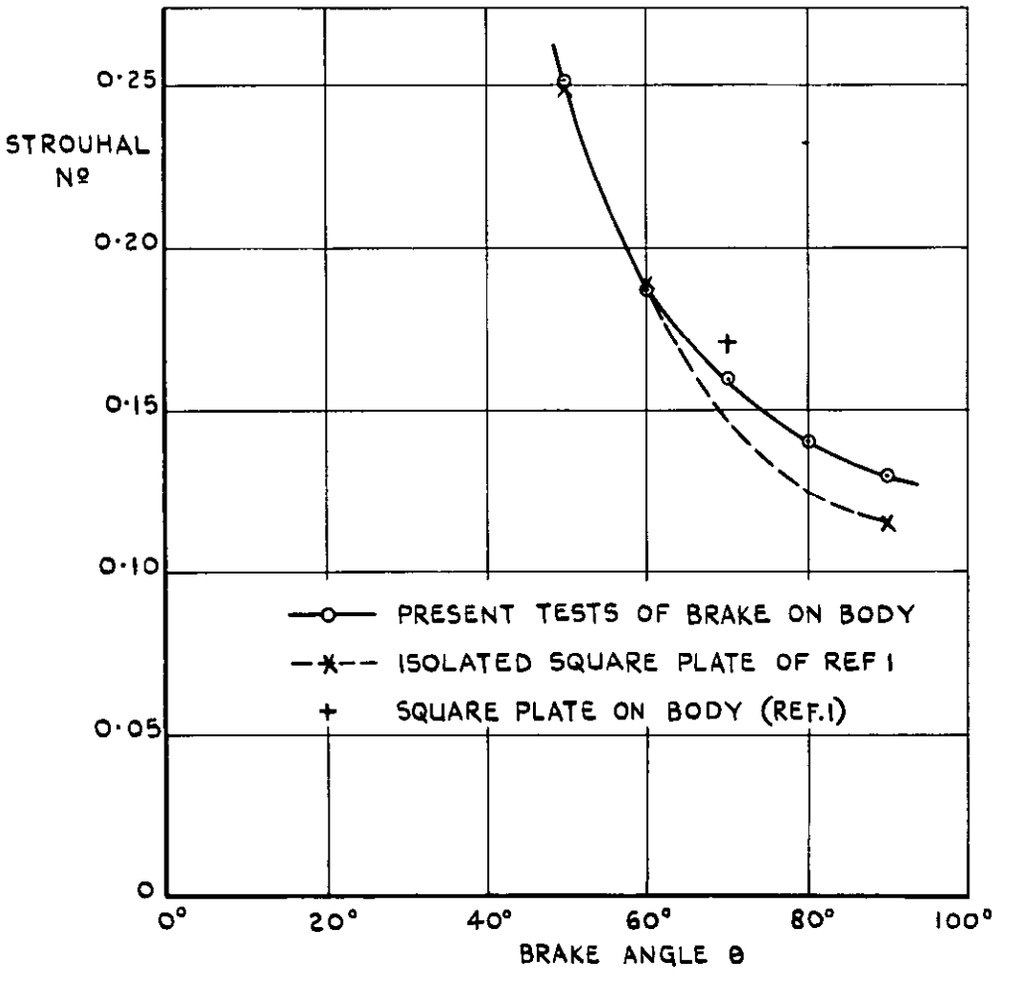

FIG.8. VARIATION OF STROUHAL NUMBER WITH BRAKE ANGLE.

C.P. No. 288
(18,260)
A.R.C. Technical Report

Published by
HER MAJESTY'S STATIONERY OFFICE

To be purchased from
York House, Kingsway, London W C 2
423 Oxford Street, London W.1
P.O Box 569, London S.E.1
13A Castle Street, Edinburgh 2
109 St. Mary Street, Cardiff
39 King Street, Manchester 2
Tower Lane, Bristol 1
2 Edmund Street, Birmingham 3
80 Chichester Street, Belfast
or through any bookseller

PRINTED IN GREAT BRITAIN

S.O. Code No 23-9009-88

C.P. No. 288